

## 10 Method of Invariant Grids

The method of invariant grids is developed for a grid-based computation of invariant manifolds.

### 10.1 Invariant Grids

Elsewhere above in this book, we considered the immersions  $F(y)$ , and the methods for their construction, without addressing the question of how to implement  $F$  numerically. In most of the works (of us and of other people on similar problems), analytic forms were required to represent manifolds (see, however, the method of Legendre integrators [254, 266, 369]). However, in order to construct manifolds of a relatively low dimension, grid-based representations of manifolds become a relevant option. The *method of invariant grids* (MIG) was suggested recently in [22].

The main idea of MIG is to find a mapping of the finite-dimensional grids into the phase space of a dynamic system. That is, we construct not just a point approximation of the invariant manifold  $F^*(y)$ , but an *invariant grid*. When refined, it is expected to converge, of course, to  $F^*(y)$ , but in any case it is a separate, independently defined object.

Let's denote  $L = R^n$ ,  $G$  is a discrete subset of  $R^n$ . It is natural to think of a regular grid, but this is not so crucial. For every point  $y \in G$ , a neighborhood of  $y$  is defined:  $V_y \subset G$ , where  $V_y$  is a finite set, and, in particular,  $y \in V_y$ . On regular grids,  $V_y$  includes, as a rule, the nearest neighbors of  $y$ . It may also include the points next to the nearest neighbors.

For our purpose, we should define a grid differential operator. For every function, defined on the grid, also all derivatives are defined:

$$\left. \frac{\partial f}{\partial y_i} \right|_{y \in G} = \sum_{z \in V_y} q_i(z, y) f(z), i = 1, \dots, n. \quad (10.1)$$

where  $q_i(z, y)$  are some coefficients.

Here we do not specify the choice of the functions  $q_i(z, y)$ . We just mention in passing that, as a rule, (10.1) is established using some approximation of  $f$  in the neighborhood of  $y$  in  $R^n$  by some differentiable functions (for example, polynomials). This approximation is based on the values of  $f$  at the points of

$V_y$ . For regular grids,  $q_i(z, y)$  are functions of the difference  $z - y$ . For some of the nodes  $y$  which are close to the edges of the grid, functions are defined only on the part of  $V_y$ . In this case, the coefficients in (10.1) should be modified appropriately in order to provide an approximation using available values of  $f$ . Below we assume this modification is always done. We also assume that the number of points in the neighborhood  $V_y$  is always sufficient to make the approximation possible. This assumption restricts the choice of the grids  $G$ . Let's call *admissible* all such subsets  $G$ , on which one can define differentiation operator in every point.

Let  $F$  be a given mapping of some admissible subset  $G \subset R^n$  into  $U$ . For every  $y \in V$  we define tangent vectors:

$$T_y = \text{Lin}\{g_i\}_1^n, \quad (10.2)$$

where vectors  $g_i (i = 1, \dots, n)$  are partial derivatives (10.1) of the vector-function  $F$ :

$$g_i = \frac{\partial F}{\partial y_i} = \sum_{z \in V_y} q_i(z, y) F(z), \quad (10.3)$$

or in the coordinate form:

$$(g_i)_j = \frac{\partial F_j}{\partial y_i} = \sum_{z \in V_y} q_i(z, y) F_j(z). \quad (10.4)$$

Here  $(g_i)_j$  is the  $j$ th coordinate of the vector  $(g_i)$ , and  $F_j(z)$  is the  $j$ th coordinate of the point  $F(z)$ .

The grid  $G$  is *invariant*, if for every node  $y \in G$  the vector field  $J(F(y))$  belongs to the tangent space  $T_y$  (here  $J$  is the right hand side of the kinetic equations (3.1)).

So, the definition of the invariant grid includes:

1. The finite admissible subset  $G \subset R^n$ ;
2. A mapping  $F$  of this admissible subset  $G$  into  $U$  (where  $U$  is the phase space of kinetic equation (3.1));
3. The differentiation formulas (10.1) with given coefficients  $q_i(z, y)$ ;

The *grid invariance equation* has a form of an inclusion:

$$J(F(y)) \in T_y \text{ for every } y \in G,$$

or a form of an equation:

$$(1 - P_y)J(F(y)) = 0 \text{ for every } y \in G,$$

where  $P_y$  is the thermodynamic projector (5.25).

The grid differentiation formulas (10.1) are needed, in the first place, to establish the tangent space  $T_y$ , and the null space of the thermodynamic projector  $P_y$  in each node. It is important to realize that the locality of the

construction of the thermodynamic projector enables this without a global parametrization.

Basically, in our approach, the grid specifics is in: (a) differentiation formulas, (b) grid construction strategy (the grid can be extended, contracted, refined, etc.) The invariance equations (3.3), equations of the film dynamics extension (4.5), the iteration Newton method (6.2), and the formulae of the relaxation approximation (9.2) do not change at all. For convenience, let us rewrite all these formulas in the grid context.

Let  $x = F(y)$  be the location of the grid's node  $y$  immersed into  $U$ . We have the set of tangent vectors  $g_i(x)$ , defined in  $x$  (10.3), (10.4). Thus, the tangent space  $T_y$  is defined by (10.2). Also, one has the entropy function  $S(x)$ , the linear functional  $D_x S|_x$ , and the subspace  $T_{0y} = T_y \cap \ker D_x S|_x$  in  $T_y$ . Let  $T_{0y} \neq T_y$ . In this case we have a vector  $e_y \in T_y$ , orthogonal to  $T_{0y}$ ,  $D_x S|_x(e_y) = 1$ . Then the thermodynamic projector is defined as:

$$P_y \bullet = P_{0y} \bullet + e_y D_x S|_x \bullet, \quad (10.5)$$

where  $P_{0y}$  is the orthogonal projector on  $T_{0y}$  with respect to the entropic scalar product  $\langle | \rangle_x$ .

If  $T_{0y} = T_y$ , then the thermodynamic projector is the orthogonal projector on  $T_y$  with respect to the entropic scalar product  $\langle | \rangle_x$ .

For the Newton method with incomplete linearization, the equations for calculation the new node location  $x' = x + \delta x$  are:

$$\begin{cases} P_y \delta x = 0 \\ (1 - P_y)(J(x) + DJ(x)\delta x) = 0. \end{cases} \quad (10.6)$$

Here  $DJ(x)$  is a matrix of derivatives of  $J$  evaluated at  $x$ . The self-adjoint linearization can be used too (see Chap. 7).

Equation (10.6) is a system of linear algebraic equations. In practice, it proves convenient to choose some orthonormal (with respect to the entropic scalar product) basis  $\mathbf{b}_i$  in  $\ker P_y$ . Let  $r = \dim(\ker P_y)$ . Then  $\delta x = \sum_{i=1}^r \delta_i \mathbf{b}_i$ , and system (10.6) takes the form

$$\sum_{k=1}^r \delta_k \langle \mathbf{b}_i | DJ(x) \mathbf{b}_k \rangle_x = -\langle J(x) | \mathbf{b}_i \rangle_x, i = 1 \dots r. \quad (10.7)$$

This is the system of linear equations for adjusting the node location according to the Newton method with incomplete linearization.

For the relaxation method, one needs to calculate the defect  $\Delta_x = (1 - P_y)J(x)$ , and the relaxation step

$$\tau(x) = -\frac{\langle \Delta_x | \Delta_x \rangle_x}{\langle \Delta_x | DJ(x) \Delta_x \rangle_x}. \quad (10.8)$$

Then, the new node location  $x'$  is computed as

$$x' = x + \tau(x)\Delta_x . \quad (10.9)$$

This is the equation for adjusting the node location according to the relaxation method.

## 10.2 Grid Construction Strategy

From all the reasonable strategies of the invariant grid construction we consider here the following two: the *growing lump* and the *invariant flag*.

### 10.2.1 Growing Lump

The construction is initialized from the equilibrium point  $y^*$ . The first approximation is constructed as  $F(y^*) = x^*$ , and for some initial  $V_0$  ( $V_{y^*} \subset V_0$ ) one has  $F(y) = x^* + A(y - y^*)$ , where  $A$  is an isometric embedding (in the standard Euclidean metrics) of  $R^n$  in  $E$ .

For this initial grid one makes a fixed number of iterations of one of the methods chosen (Newton's method with incomplete linearization or the relaxation method), and, after that, puts  $V_1 = \bigcup_{y \in V_0} V_y$  and extends  $F$  from  $V_0$  onto  $V_1$  using the linear extrapolation, and the process continues. One of the possible variants of this procedure is to extend the grid from  $V_i$  to  $V_{i+1}$  not after a fixed number of iterations, but only after the invariance defect  $\Delta_y$  becomes less than a given  $\epsilon$  (in a given norm, which is entropic, as a rule), for all nodes  $y \in V_i$ . The lump stops growing after it reaches the boundary and is within a given accuracy  $\|\Delta\| < \epsilon$ .

### 10.2.2 Invariant Flag

In order to construct the invariant flag one uses sufficiently regular grids  $G$ , in which many points are located on the coordinate lines, planes, etc. One considers the standard flag  $R^0 \subset R^1 \subset R^2 \subset \dots \subset R^n$  (every next space is constructed by adding one more coordinate). It corresponds to a sequence of grids  $\{y^*\} \subset G^1 \subset G^2 \dots \subset G^n$ , where  $\{y^*\} = R^0$ , and  $G^i$  is a grid in  $R^i$ .

First,  $y^*$  is mapped on  $x^*$  and further  $F(y^*) = x^*$ . Then the invariant grid is constructed on  $V^1 \subset G^1$  (up to the boundaries and within a given accuracy  $\|\Delta\| < \epsilon$ ). After that, the neighborhoods in  $G^2$  are added to the points  $V^1$ , and the grid  $V^2 \subset G^2$  is constructed (up to the boundaries and within a given accuracy) and so on, until  $V^n \subset G^n$  is constructed.

While constructing the  $k$ th-order grid  $V^k \subset G^k$ , the important role of the grids of lower dimension  $V^0 \subset \dots \subset V^{k-1} \subset V^k$  embedded in it, is preserved. The point  $F(y^*) = x^*$  (equilibrium) remains fixed. For every  $y \in V^q$  ( $q < k$ ) the tangent vectors  $g_1, \dots, g_q$  are constructed, using the differentiation operators (10.1) on the whole  $V^k$ . Using the tangent space  $T_y = \text{Lin}\{g_1, \dots, g_q\}$ ,

the projector  $P_y$  is constructed, the iterations are applied and so on. All this is done in order to obtain a sequence of embedded invariant grids, given by the same map  $F$ .

### 10.2.3 Boundaries Check and the Entropy

We construct grid mapping of  $F$  onto a finite set  $V \in G$ . The technique of checking whether the grid still belongs to the phase space  $U$  of the kinetic system ( $F(V) \subset U$ ) is quite straightforward: all the points  $y \in V$  are checked whether they belong to  $U$ . If at the next iteration a point  $F(y)$  leaves  $U$ , then it is pulled inside by a homothety transform with the center in  $x^*$ . Since the entropy is a concave function, the homothety contraction with the center in  $x^*$  increases the entropy monotonically. Another variant to cut off the points which leave  $U$ .

By construction (5.25), the kernel of the entropic projector is annulled by the entropy differential. Thus, in the first order, the steps in the Newton method with incomplete linearization (6.2) as well as in the relaxation method (9.1), (9.2) do not change the entropy. But if the steps are quite large, then the increase of the entropy may become essential, and the points are returned on their entropy levels by the homothety contraction with the center in the equilibrium point.

## 10.3 Instability of Fine Grids

When one reduces the grid spacing in order to refine the grid, then, once the grid spacing becomes small enough, one can face the problem of the *Courant instability* [269–271]. Instead of converging, at every iteration the grid becomes more and more entangled (see Fig. 10.1).

A way to avoid such instability is well-known. This is decreasing the time step. In our problem, instead of a true time step, we have a shift in the Newtonian direction. Formally, we can assign the value  $h = 1$  for one complete step in the Newtonian direction. Let us extend now the Newton method to arbitrary  $h$ . For this, let us find  $\delta x = \delta F(y)$  from (10.6), but update  $\delta x$  proportionally to  $h$ ; the new value of  $x_{n+1} = F_{n+1}(y)$  is equal to

$$F_{n+1}(y) = F_n(y) + h_n \delta F_n(y) \quad (10.10)$$

where  $n$  denotes the number of iteration.

One way to choose the step value  $h$  is to make it adaptive, by controlling the average value of the invariance defect  $\|\Delta_y\|$  at every step. Another way is the convergence control: then  $\sum h_n$  plays a role of time.

Elimination of the Courant instability for the relaxation method can be done quite analogously. Everywhere the step  $h$  is maintained as large as it is possible without running into convergence problems.

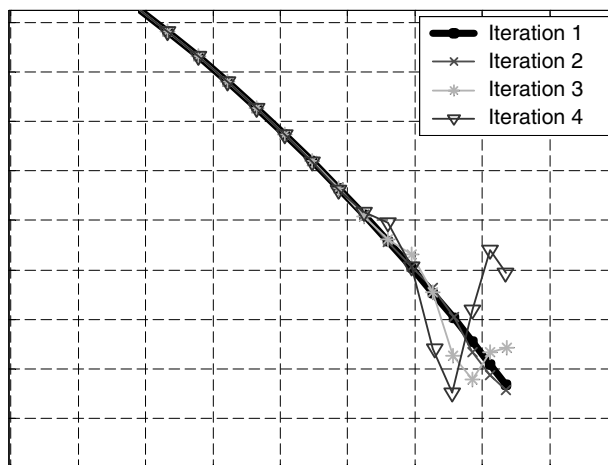


**Fig. 10.1.** Grid instability. For small grid steps approximations in the calculation of grid derivatives lead to the grid instability effect. Several successive iterations of the algorithm without adaptation of the time step are shown that lead to undesirable “oscillations”, which eventually destroy the grid starting from one of its ends

#### 10.4 Which Space is Most Appropriate for the Grid Construction?

For kinetic systems, there are two distinguished representations of the phase space:

- The density space (concentrations, energy or probability densities, etc.)
- The space of conjugated intensive variables, (temperature, chemical potentials, etc.)

The density space is convenient for the construction of the quasi-chemical representations. Here the balance relations are linear and the constraints are in the form of linear inequalities (the densities themselves or some of their linear combinations must be positive).

The conjugated variables space is convenient in the sense that the equilibrium conditions are linear in terms of the conjugate variables. In these spaces the quasiequilibrium manifolds exist in the form of linear subspaces and, vice versa, linear balance equations turn out to be equations of the conditional entropy maximum.

The duality we have just mentioned is well-known and studied in detail in many works on thermodynamics and Legendre transformation [274,275]. This viewpoint of nonequilibrium thermodynamics unifies many well-established mesoscopic dynamical theories, as for example the Boltzmann kinetic theory and the Navier–Stokes–Fourier hydrodynamics [189]. To this end, preceding the grids in the density space were discussed. However, the use of the space

of conjugated variables seems to be even more appealing for the grid construction. The main argument is the specific role of quasiequilibrium, which is a linear manifold in the conjugated space. Therefore, a linear extrapolation gives a thermodynamically justified quasiequilibrium approximation. A linear approximation of the slow invariant manifold in the neighborhood of the equilibrium in terms of the conjugate variables space already gives the readily global quasiequilibrium manifold which corresponds to the motion separation in the neighborhood of the equilibrium point.

For the mass action law, transition to the conjugate variables is simply the logarithmic transformation of the coordinates.

### 10.5 Carleman's Formula in the Analytical Invariant Manifolds Approximations. First Benefit of Analyticity: Superresolution

When constructing invariant grids, one must define the differential operators (10.1) for every grid's node. For calculating the differential operators in some point  $y$ , an interpolation procedure in the neighborhood of  $y$  is used. As a rule, it is an interpolation by a low-order polynomial, which is constructed using the function values in the nodes belonging to the neighbourhood of  $y$  in  $G$ . This approximation (using values in the nearest neighborhood nodes) is natural for smooth functions. But we are looking for the *analytical* invariant manifold (see discussion in Chap. 4). Analytical functions have a much more "rigid" structure than the smooth ones. One can change a smooth function in the neighborhood of any point in such a way, that outside this neighborhood the function will not change. In general, this is not possible for analytical functions: a kind of a "long-range" effect takes place (as is well known).

The idea is to make use of this effect and to reconstruct some analytical function  $f_G$  using a function given on  $G$ . There is one important requirement: if the values given on  $G$  are values of some function  $f$  which is analytical in a neighborhood  $U$ , then, if the  $G$  is refined "correctly", one must have  $f_G \rightarrow f$  in  $U$ . The sequence of reconstructed function  $f_G$  should converge to the "right" function  $f$ .

What is the "correct refinement"? For smooth functions for the convergence  $f_G \rightarrow f$  it is necessary and sufficient that, in the course of refinement,  $G$  would approximate the whole  $U$  with arbitrary accuracy. For analytical functions it is necessary only that, under the refinement,  $G$  would approximate some uniqueness set<sup>1</sup>  $A \subset U$ . Suppose we have a sequence of grids  $G$ , each next is finer than the previous, which approximate a set  $A$ . For smooth functions using function values defined on the grids one can reconstruct the function in  $A$ . For analytical functions, if the analyticity domain  $U$  is known, and

<sup>1</sup> Let's remind to the reader that  $A \subset U$  is called *uniqueness set* in  $U$  if for analytical in  $U$  functions  $\psi$  and  $\varphi$  from  $\psi|_A \equiv \varphi|_A$  it follows  $\psi \equiv \varphi$ .

$A$  is a uniqueness set in  $U$ , then one can reconstruct the function in  $U$ . The set  $U$  can be essentially bigger than  $A$ ; because of this such extension was named as *superresolution effect* [276]. There exist formulas for construction of analytical functions  $f_G$  for different domains  $U$ , uniqueness sets  $A \subset U$  and for different ways of discrete approximation of  $A$  by a sequence of refined grids  $G$  [276]. Here we provide only one Carleman's formula which is the most appropriate for our purposes.

Let domain  $U = Q_\sigma^n \subset C^n$  be a product of strips  $Q_\sigma \subset C$ ,  $Q_\sigma = \{z | \text{Im}z < \sigma\}$ . We shall construct functions holomorphic in  $Q_\sigma^n$ . This is effectively equivalent to the construction of real analytical functions  $f$  in the whole  $R^n$  with a condition on the convergence radius  $r(x)$  of the Taylor series for  $f$  as a function of each coordinate:  $r(x) \geq \sigma$  in every point  $x \in R^n$ .

The sequence of refined grids is constructed as follows: let for every  $l = 1, \dots, n$  a finite sequence of distinct points  $N_l \subset Q_\sigma$  be defined:

$$N_l = \{x_{lj} | j = 1, 2, 3 \dots\}, x_{lj} \neq x_{li} \text{ for } i \neq j \tag{10.11}$$

The countable uniqueness set  $A$ , which is approximated by a sequence of refined grids, has the form:

$$A = N_1 \times N_2 \times \dots \times N_n = \{(x_{1i_1}, x_{2i_2}, \dots, x_{ni_n}) | i_1, \dots, i_n = 1, 2, 3, \dots\} \tag{10.12}$$

The grid  $G_m$  is defined as the product of initial fragments  $N_l$  of length  $m$ :

$$G_m = \{(x_{1i_1}, x_{2i_2} \dots x_{ni_n}) | 1 \leq i_1, \dots, i_n \leq m\} \tag{10.13}$$

Let us denote  $\lambda = 2\sigma/\pi$  ( $\sigma$  is a half-width of the strip  $Q_\sigma$ ). The key role in the construction of the Carleman's formula is played by the functional  $\omega_m^\lambda(u, p, l)$  of 3 variables:  $u \in U = Q_\sigma^n$ ,  $p$  is an integer,  $1 \leq p \leq m$ ,  $l$  is an integer,  $1 \leq l \leq n$ . Further  $u$  will be the coordinate value at the point where the extrapolation is calculated,  $l$  will be the coordinate number, and  $p$  will be an element of multi-index  $\{i_1, \dots, i_n\}$  for the point  $(x_{1i_1}, x_{2i_2}, \dots, x_{ni_n}) \in G$ :

$$\begin{aligned} \omega_m^\lambda(u, p, l) &= \frac{(e^{\lambda x_{lp}} + e^{\lambda \bar{x}_{lp}})(e^{\lambda u} - e^{\lambda x_{lp}})}{\lambda(e^{\lambda u} + e^{\lambda \bar{x}_{lp}})(u - x_{lp})e^{\lambda x_{lp}}} \\ &\times \prod_{j=1, j \neq p}^m \frac{(e^{\lambda x_{lp}} + e^{\lambda \bar{x}_{lj}})(e^{\lambda u} - e^{\lambda x_{lj}})}{(e^{\lambda x_{lp}} - e^{\lambda x_{lj}})(e^{\lambda u} + e^{\lambda \bar{x}_{lj}})} \end{aligned} \tag{10.14}$$

For real-valued  $x_{pk}$  formula (10.14) simplifies:

$$\omega_m^\lambda(u, p, l) = 2 \frac{e^{\lambda u} - e^{\lambda x_{lp}}}{\lambda(e^{\lambda u} + e^{\lambda x_{lp}})(u - x_{lp})} \times \prod_{j=1, j \neq p}^m \frac{(e^{\lambda x_{lp}} + e^{\lambda x_{lj}})(e^{\lambda u} - e^{\lambda x_{lj}})}{(e^{\lambda x_{lp}} - e^{\lambda x_{lj}})(e^{\lambda u} + e^{\lambda x_{lj}})} \tag{10.15}$$

The Carleman formula for extrapolation from  $G_M$  on  $U = Q_\sigma^n$  ( $\sigma = \pi\lambda/2$ ) has the form ( $z = (z_1, \dots, z_n)$ ):

$$f_m(z) = \sum_{k_1, \dots, k_n=1}^m f(x_k) \prod_{j=1}^n \omega_m^\lambda(z_j, k_j, j), \quad (10.16)$$

where  $k = k_1, \dots, k_n$ ,  $x_k = (x_{1k_1}, x_{2k_2}, \dots, x_{nk_n})$ .

There exists a theorem [276]:

If  $f \in H^2(Q_\sigma^n)$ , then  $f(z) = \lim_{m \rightarrow \infty} f_m(z)$ , where  $H^2(Q_\sigma^n)$  is the Hardy class of holomorphic in  $Q_\sigma^n$  functions.

It is useful to present the asymptotics of (10.16) for large  $|\operatorname{Re}z_j|$ . For this purpose, we shall consider the asymptotics of (10.16) for large  $|\operatorname{Re}u|$ :

$$|\omega_m^\lambda(u, p, l)| = \left| \frac{2}{\lambda u} \prod_{j=1, j \neq p}^m \frac{e^{\lambda x_{lp}} + e^{\lambda x_{lj}}}{e^{\lambda x_{lp}} - e^{\lambda x_{lj}}} \right| + o(|\operatorname{Re}u|^{-1}). \quad (10.17)$$

From the formula (10.16) one can see that for the finite  $m$  and  $|\operatorname{Re}z_j| \rightarrow \infty$  function  $|f_m(z)|$  behaves like  $\text{const} \cdot \prod_j |z_j|^{-1}$ .

This property (zero asymptotics) must be taken into account when using the formula (10.16). When constructing invariant manifolds  $F(W)$ , it is natural to use (10.16) not for the immersion  $F(y)$ , but for the deviation of  $F(y)$  from some analytical ansatz  $F_0(y)$  [277–280].

The analytical ansatz  $F_0(y)$  can be obtained using Taylor series, just as in the Lyapunov auxiliary theorem [3] (see also Chap. 4). Another variant is to use Taylor series for the construction of Pade-approximations.

It is natural to use approximations (10.16) in terms of dual variables as well, since there exists for them (as the examples demonstrate) a simple and effective linear ansatz for the invariant manifold. This is the slow invariant subspace  $E_{\text{slow}}$  of the operator of linearized system (3.1) in dual variables at the equilibrium point. This invariant subspace corresponds to the set of “slow” eigenvalues (with small  $|\operatorname{Re}\lambda|$ ,  $\operatorname{Re}\lambda < 0$ ). In the space of concentrations this invariant subspace is the quasiequilibrium manifold. It consists of the maximum entropy points on the affine manifolds of the form  $x + E_{\text{fast}}$ , where  $E_{\text{fast}}$  is the “fast” invariant subspace of the operator of the linearized system (3.1) at the equilibrium point. It corresponds to the “fast” eigenvalues (large  $|\operatorname{Re}\lambda|$ ,  $\operatorname{Re}\lambda < 0$ ).

Carleman’s formulas can be useful for the invariant grids construction in two places: first, for the definition of the grid differential operators (10.1), and second, for the analytical continuation of the manifold from the grid.

## 10.6 Example: Two-Step Catalytic Reaction

Let us consider a two-step four-component reaction with one catalyst  $A_2$  (the Michaelis-Menten mechanism):



We assume the Lyapunov function of the form

$$S = -G = -\sum_{i=1}^4 c_i [\ln(c_i/c_i^{\text{eq}}) - 1].$$

The kinetic equation for the four-component vector of concentrations,  $\mathbf{c} = (c_1, c_2, c_3, c_4)$ , has the form

$$\dot{\mathbf{c}} = \gamma_1 W_1 + \gamma_2 W_2. \quad (10.19)$$

Here  $\gamma_{1,2}$  are stoichiometric vectors,

$$\gamma_1 = (-1, -1, 1, 0), \quad \gamma_2 = (0, 1, -1, 1), \quad (10.20)$$

while functions  $W_{1,2}$  are reaction rates:

$$W_1 = k_1^+ c_1 c_2 - k_1^- c_3, \quad W_2 = k_2^+ c_3 - k_2^- c_2 c_4. \quad (10.21)$$

Here  $k_{1,2}^\pm$  are reaction rate constants. The system under consideration has two conservation laws,

$$c_1 + c_3 + c_4 = B_1, \quad c_2 + c_3 = B_2, \quad (10.22)$$

or  $\langle \mathbf{b}_{1,2}, \mathbf{c} \rangle = B_{1,2}$ , where  $\mathbf{b}_1 = (1, 0, 1, 1)$  and  $\mathbf{b}_2 = (0, 1, 1, 0)$ . The nonlinear system (10.18) is effectively two-dimensional, and we consider a one-dimensional reduced description. For our example, we chose the following set of parameters:

$$\begin{aligned} k_1^+ &= 0.3, \quad k_1^- = 0.15, \quad k_2^+ = 0.8, \quad k_2^- = 2.0; \\ c_1^{\text{eq}} &= 0.5, \quad c_2^{\text{eq}} = 0.1, \quad c_3^{\text{eq}} = 0.1, \quad c_4^{\text{eq}} = 0.4; \\ B_1 &= 1.0, \quad B_2 = 0.2 \end{aligned} \quad (10.23)$$

The one-dimensional invariant grid is shown in Fig. 10.2 in the  $(c_1, c_4, c_3)$  coordinates. The grid was constructed by the growing lump method, as described above. We used Newton iterations to adjust the nodes. The grid was grown up to the boundaries of the phase space.

The grid in this example is a one-dimensional ordered sequence  $\{x_1, \dots, x_n\}$ . The grid derivatives for calculating the tangent vectors  $g$  were taken as  $g(x_i) = (x_{i+1} - x_{i-1}) / \|x_{i+1} - x_{i-1}\|$  for the internal nodes, and  $g(x_1) = (x_1 - x_2) / \|x_1 - x_2\|$ ,  $g(x_n) = (x_n - x_{n-1}) / \|x_n - x_{n-1}\|$  for the grid's boundaries.

Close to the phase space boundaries we had to apply an adaptive algorithm for choosing the time step  $h$ : if, after the next growing step (adding new nodes to the grid and after completing  $N = 20$  Newtonian steps, the grid did not converged, then we choose a new step size  $h_{n+1} = h_n/2$  and recalculate the grid. The final (minimal) value for  $h$  was  $h \approx 0.001$ .

The location of the nodes was parametrized with the entropic distance to the equilibrium point measured in the quadratic metrics given by the matrix

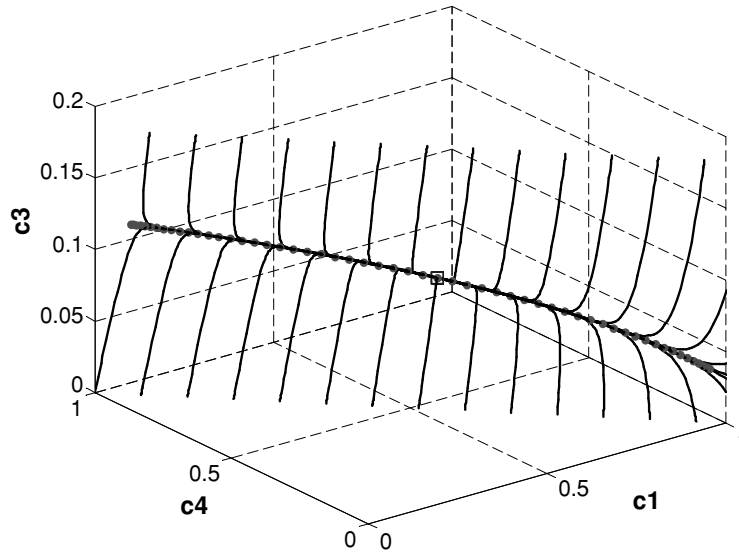


**Fig. 10.2.** One-dimensional invariant grid (*circles*) for the two-dimensional chemical system. Projection into the 3d-space of  $c_1$ ,  $c_4$ ,  $c_3$  concentrations. The trajectories of the system in the phase space are shown by lines. The equilibrium point is marked by the square. The system quickly reaches the grid and further moves along it

$H_c = -\|\partial^2 S(c)/\partial c_i \partial c_j\|$  in the equilibrium  $c^{eq}$ . It means that every node is located on a sphere in this metrics with a given radius, which increases linearly with number of the node. In this figure the step of the increase is chosen to be 0.05. Thus, the first node is at the distance 0.05 from the equilibrium, the second is at the distance 0.10 and so on. Figure 10.3 shows several important quantities which facilitate understanding of the object (invariant grid) extracted. The sign on the x-axis of the graphs at Fig. 10.3 is meaningless since the distance is always positive, but in this situation it indicates two possible directions from the equilibrium point.

Figure 10.3a,b represents the slow one-dimensional component of the dynamics of the system. Given any initial condition, the system quickly finds the corresponding point on the manifold and starting from this point the dynamics is given by a part of the graph on the Fig. 10.3a,b.

One of the useful quantities is shown on the Fig. 10.3c. It is the relation between the relaxation times “toward” and “along” the grid ( $\lambda_2/\lambda_1$ , where  $\lambda_1$ ,  $\lambda_2$  are the smallest and the next smallest by absolute value non-zero eigenvalue of the system, symmetrically linearized at the point of the grid node). The figure demonstrates that the system is very stiff close to the equilibrium point ( $\lambda_1$  and  $\lambda_2$  are well separated from each other), and becomes less stiff (by order of magnitude) near the boundary. This leads to the conclusion that the one-dimensional reduced model is more adequate in the neighborhood

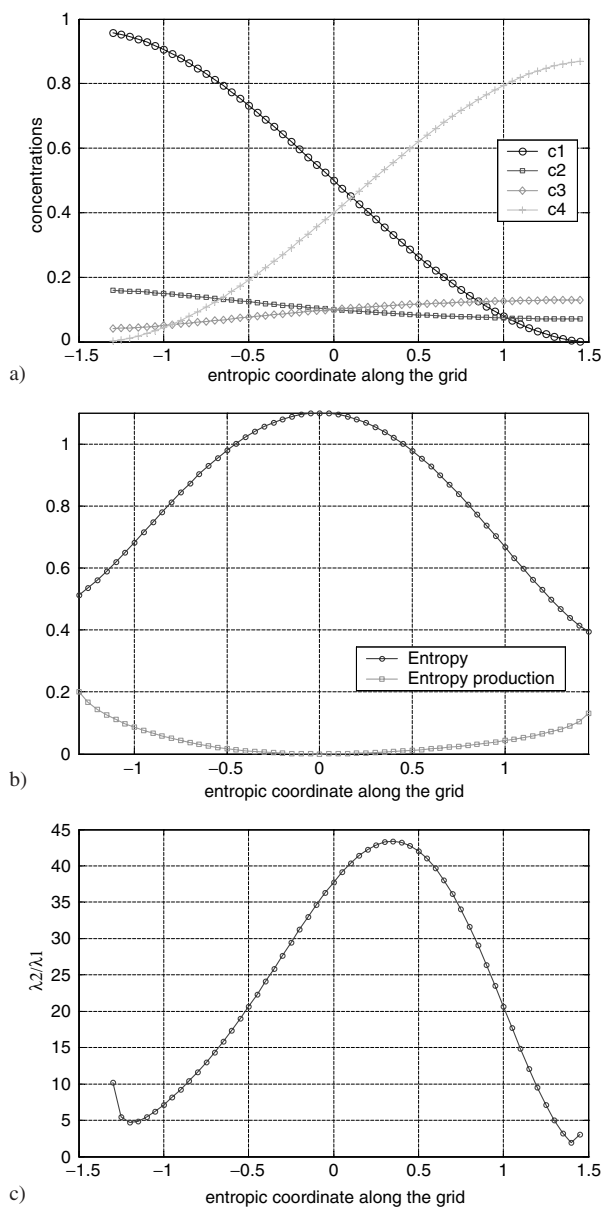


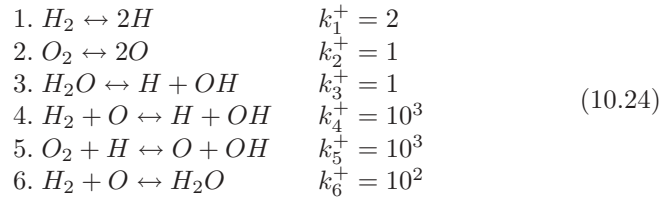
**Fig. 10.3.** One-dimensional invariant grid for the two-dimensional chemical system. (a) Values of the concentrations along the grid. (b) Values of the entropy and the entropy production ( $-dG/dt$ ) along the grid. (c) Ratio of the relaxation times “towards” and “along” the manifold. The nodes positions are parametrized with entropic distance measured in the quadratic metrics given by  $\mathbf{H}_c = -\|\partial^2 S(c)/\partial c_i \partial c_j\|$  in the equilibrium  $c^{eq}$ . Entropic coordinate equal to zero corresponds to the equilibrium

of the equilibrium where fast and slow motions are separated by two orders of magnitude. On the end-points of the grid the one-dimensional reduction ceases to be well-defined.

## 10.7 Example: Model Hydrogen Burning Reaction

In this section we consider a more complicated example, where the concentration space is 6-dimensional, while the system is 4-dimensional. We construct an invariant flag which consists of 1- and 2-dimensional invariant manifolds.

We consider a chemical system with six species called  $H_2$  (hydrogen),  $O_2$  (oxygen),  $H_2O$  (water),  $H$ ,  $O$ ,  $OH$  (radicals). We assume the Lyapunov function of the form  $S = -G = -\sum_{i=1}^6 c_i [\ln(c_i/c_i^{\text{eq}}) - 1]$ . The subset of the hydrogen burning reaction and corresponding (direct) rate constants have were taken as:



The conservation laws are:

$$\begin{array}{l}
 2c_{H_2} + 2c_{H_2O} + c_H + c_{OH} = b_H \\
 2c_{O_2} + c_{H_2O} + c_O + c_{OH} = b_O
 \end{array} \quad (10.25)$$

For parameter values we took  $b_H = 2$ ,  $b_O = 1$ , and the equilibrium point:

$$c_{H_2}^{\text{eq}} = 0.27 \quad c_{O_2}^{\text{eq}} = 0.135 \quad c_{H_2O}^{\text{eq}} = 0.7 \quad c_H^{\text{eq}} = 0.05 \quad c_O^{\text{eq}} = 0.02 \quad c_{OH}^{\text{eq}} = 0.01 \quad (10.26)$$

Other rate constants  $k_i^-$ ,  $i = 1 \dots 6$  were calculated from  $c^{\text{eq}}$  value and  $k_i^+$ . For this system the stoichiometric vectors are:

$$\begin{array}{ll}
 \gamma_1 = (-1, 0, 0, 2, 0, 0) & \gamma_2 = (0, -1, 0, 0, 2, 0) \\
 \gamma_3 = (0, 0, -1, 1, 0, 1) & \gamma_4 = (-1, 0, 0, 1, -1, 1) \\
 \gamma_5 = (0, -1, 0, -1, 1, 1) & \gamma_6 = (-1, 0, 1, 0, -1, 0)
 \end{array} \quad (10.27)$$

The system under consideration is fictitious in the sense that the subset of equations corresponds to the simplified picture of this chemical process and the rate constants do not correspond to any experimentally measured quantities, rather they reflect only orders of magnitudes relevant real-world systems. In that sense we consider here a qualitative model system, which allows us to illustrate the invariant grids method. Nevertheless, modeling of more realistic systems differs only in the number of species and equations. This leads, of course, to computationally harder problems, but difficulties are not crucial.

Figure 10.4a presents a one-dimensional invariant grid constructed for the system. Figure 10.4b demonstrates the reduced dynamics along the manifold (for the explanation of the meaning of the  $x$ -coordinate, see the previous subsection). In Fig. 10.4c the three smallest by the absolute value non-zero eigenvalues of the symmetrically linearized Jacobian matrix of the system are shown. One can see that the two smallest eigenvalues almost interchange on one of the grid ends. This means that the one-dimensional “slow” manifold faces definite problems in this region, it is just not well defined there. In practice, it means that one has to use at least a two-dimensional grids there.

Figure 10.5a gives a view of the two-dimensional invariant grid, constructed for the system, using the “invariant flag” strategy. The grid was raised starting from the 1D-grid constructed at the previous step. At the first iteration for every node of the initial grid, two nodes (and two edges) were added. The direction of the step was chosen as the direction of the eigenvector of the matrix  $A^{sym}$  (at the point of the node), corresponding to the second “slowest” direction. The value of the step was chosen to be  $\epsilon = 0.05$  in terms of entropic distance. After several Newton’s iterations done until convergence was reached, new nodes were added in the direction “ortogonal” to the 1D-grid. This time it was done by linear extrapolation of the grid on the same step  $\epsilon = 0.05$ . Once some new nodes become one or several negative coordinates (the grid reaches the boundaries) they were cut off. If a new node has only one edge, connecting it to the grid, it was excluded (since it was impossible to calculate 2D-tangent space for this node). The process was continued until the expansion was possible (the ultimate state is when every new node had to be cut off).

The method for calculating tangent vectors for this regular rectangular 2D-grid was chosen to be quite simple. The grid consists of *rows*, which are co-oriented by construction to the initial 1D-grid, and *columns* that consist of the adjacent nodes in the neighboring rows. The direction of the columns corresponds to the second slowest direction along the grid. Then, every row and column is considered as a 1D-grid, and the corresponding tangent vectors are calculated as it was described before:

$$g_{row}(x_{k,i}) = (x_{k,i+1} - x_{k,i-1}) / \|x_{k,i+1} - x_{k,i-1}\|$$

for the internal nodes and

$$\begin{aligned} g_{row}(x_{k,1}) &= (x_{k,1} - x_{k,2}) / \|x_{k,1} - x_{k,2}\|, g_{row}(x_{k,n_k}) \\ &= (x_{k,n_k} - x_{k,n_k-1}) / \|x_{k,n_k} - x_{k,n_k-1}\| \end{aligned}$$

for the nodes which are close to the grid’s edges. Here  $x_{k,i}$  denotes the vector of the node in the  $k$ th row,  $i$ th column;  $n_k$  is the number of nodes in the  $k$ th row. Second tangent vector  $g_{col}(x_{k,i})$  is calculated analogously. In practice, it proves convenient to orthogonalize  $g_{row}(x_{k,i})$  and  $g_{col}(x_{k,i})$ .

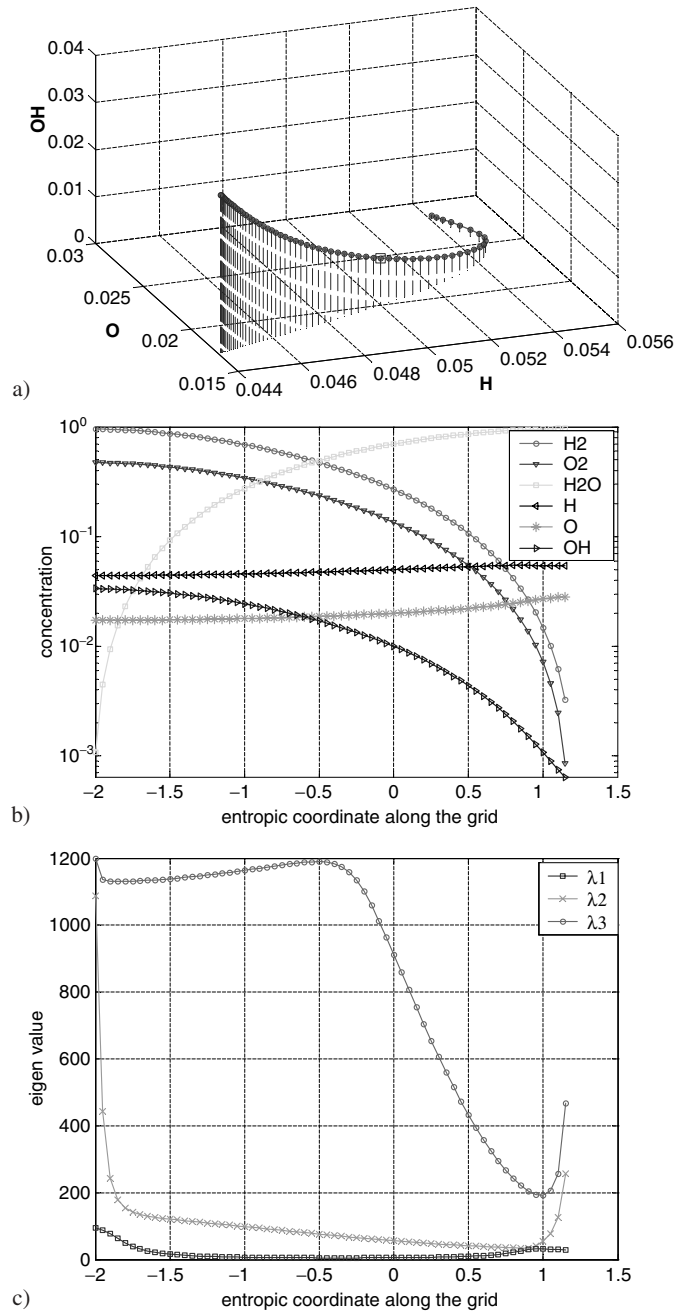
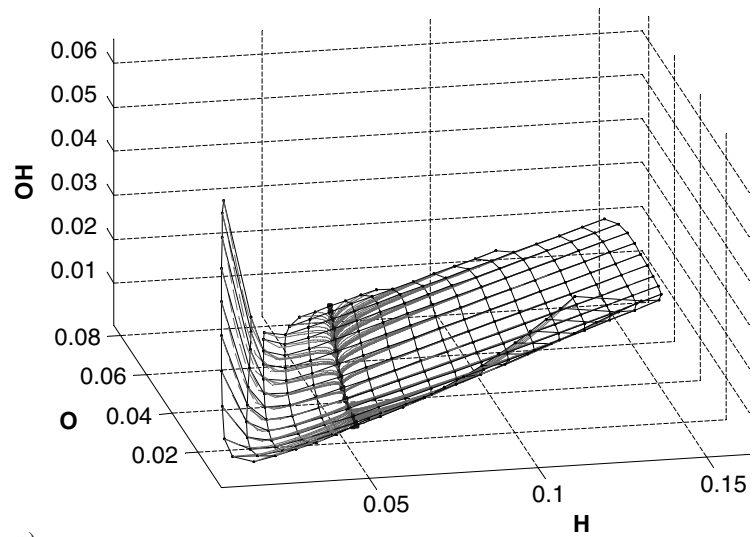
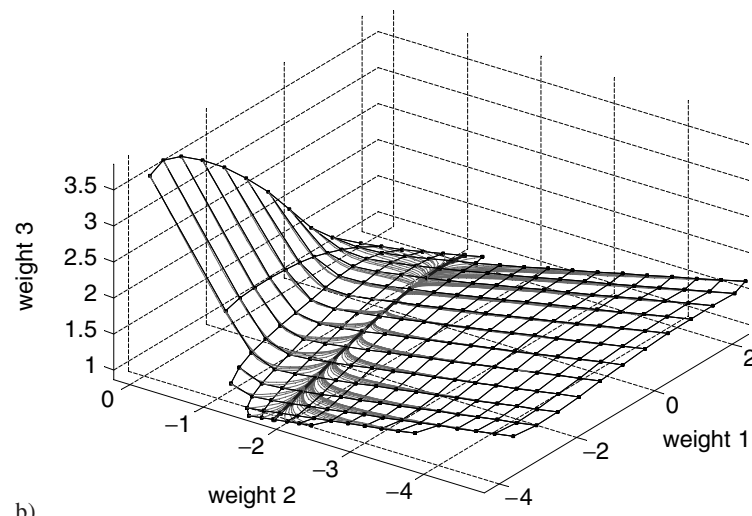


**Fig. 10.4.** One-dimensional invariant grid for model hydrogen burning reaction. (a) Projection into the 3d-space of  $c_H$ ,  $c_O$ ,  $c_{OH}$  concentrations. (b) Concentration values along the grid. (c) Three smallest by the absolute value non-zero eigenvalues of the symmetrically linearized system



a)



b)

**Fig. 10.5.** Two-dimensional invariant grid for the model hydrogen burning reaction. (a) Projection into the 3d-space of  $c_H$ ,  $c_O$ ,  $c_{OH}$  concentrations. (b) Projection into the principal 3D-subspace. Trajectories of the system are shown coming out from every node. *Bold* line denotes the one-dimensional invariant grid, starting from which the 2D-grid was constructed

## 10.8 Invariant Grid as a Tool for Data Visualization

Invariant grids provide a possibility of data visualization. In this section we demonstrate this possibility on the model hydrogen burning reaction. Since the phase space is four-dimensional, it is impossible to visualize the grid in one of the coordinate 3D-views, as it was done in the previous subsection. To facilitate visualization one can utilize traditional methods of multi-dimensional data visualization. Here we make use of the principal components analysis (see, for example, [273]), which constructs a three-dimensional linear subspace with maximal dispersion of the orthogonally projected data (grid nodes in our case). In other words, the method of principal components constructs in a multi-dimensional space a three-dimensional box such that the grid can be placed maximally tightly inside the box (in the mean square distance meaning). After projection of the grid nodes into this space, we get more or less adequate representation of the two-dimensional grid embedded into the six-dimensional concentrations space (Fig. 10.5b). The disadvantage of the approach is that the axes now do not bear any explicit physical meaning, they are just some linear combinations of the concentrations.

One attractive feature of two-dimensional grids is the possibility to use them as a screen, on which one can display different functions  $f(\mathbf{c})$  defined in the concentrations space. This technology was exploited widely in the non-linear data analysis by the elastic maps method [272]. The idea is to “unfold” the grid on a plane (to present it in the two-dimensional space, where the nodes form a regular lattice). In other words, we are going to work in the internal coordinates of the grid. In our case, the first internal coordinate (let’s call it  $s_1$ ) corresponds to the direction, co-oriented with the one-dimensional invariant grid, the second one (let us call it  $s_2$ ) corresponds to the second slow direction. By the construction, the coordinate line  $s_2 = 0$  line corresponds to the one-dimensional invariant grid. Units of  $s_1$  and  $s_2$  is the entropic distance.

Every grid node has two internal coordinates ( $s_1, s_2$ ) and, simultaneously, corresponds to a vector in the concentration space. This allows us to map any function  $f(\mathbf{c})$  from the multi-dimensional concentration space to the two-dimensional space of the grid. This mapping is defined in a finite number of points (grid nodes), and can be interpolated (linearly, in the simplest case) between them. Using *coloring* and *isolines* one can visualize the values of the function in the neighborhood of the invariant manifold. This is meaningful, since, by the definition, the system spends most of the time in the vicinity of the invariant manifold, thus, one can visualize the behavior of the system. As a result of applying this technology, one obtains a set of color illustrations (a stack of information layers), put onto the grid as a map. This enables applying the whole family of the well developed methods of working with the stack of information layers, such as the *geographical information systems* (GIS) methods.

Briefly, this technique of the visualization is a useful tool for understanding of dynamical systems. It allows to see simultaneously many different

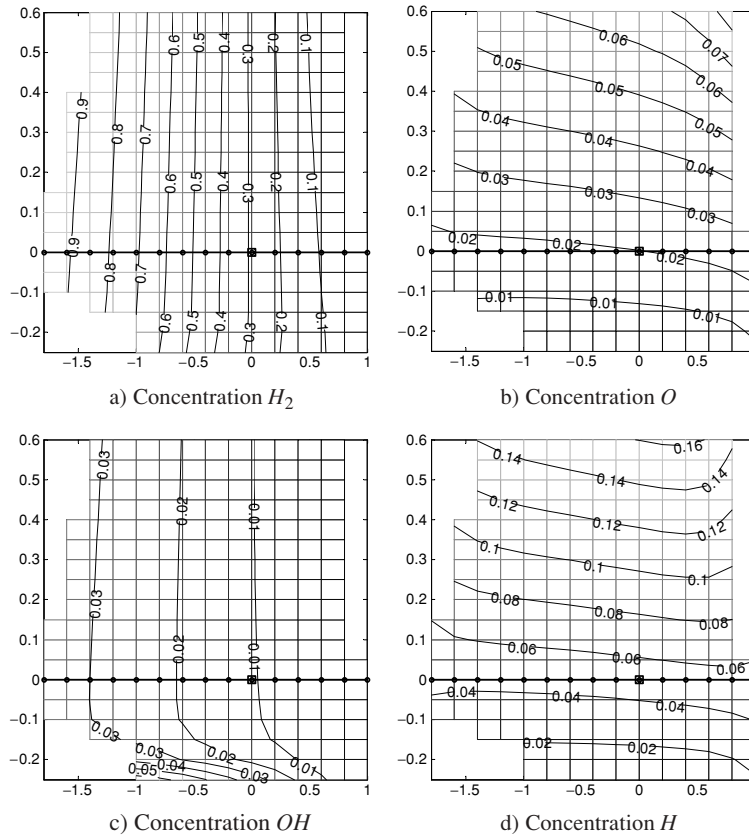


**Fig. 10.6.** Two-dimensional invariant grid as a screen for visualizing different functions defined in the concentrations space. The coordinate axes are entropic distances (see the text for the explanations) along the first and the second slowest directions on the grid. The corresponding 1D invariant grid is denoted by bold line, the equilibrium is denoted by square

scenarios of the system behavior, together with different system’s characteristics.

Let us use the invariant grids for the the model hydrogen burning system as a screen for visualisation. The simplest functions to visualize are the coordinates:  $c_i(\mathbf{c}) = c_i$ . In Fig. 10.6 we displayed four colorings, corresponding to the four arbitrarily chosen concentrations functions (of  $H_2$ ,  $O$ ,  $H$  and  $OH$ ; Fig. 10.6a-d). The qualitative conclusion that can be made from the graphs is that, for example, the concentration of  $H_2$  practically does not change during the first fast motion (towards the 1D-grid) and then, gradually changes to the equilibrium value (the  $H_2$  coordinate is “slow”). The  $O$  coordinate is the opposite case, it is the “fast” coordinate which changes quickly (on the first stage of the motion) to the almost equilibrium value, and it almost does

not change after that. Basically, the slopes of the coordinate isolines give some impression of how “slow” a given concentration is Fig. 10.6c shows an interesting behavior of the *OH* concentration. Close to the 1D grid it behaves like a “slow coordinate”, but there is a region on the map where it has a clear “fast” behavior (middle bottom of the graph).

The next two functions which one could wish to visualize are the entropy  $S$  and the entropy production  $\sigma(\mathbf{c}) = -dG/dt(\mathbf{c}) = \sum_i \ln(c_i/c_i^{eq})\dot{c}_i$ . They are shown on Fig. 10.7a,b.

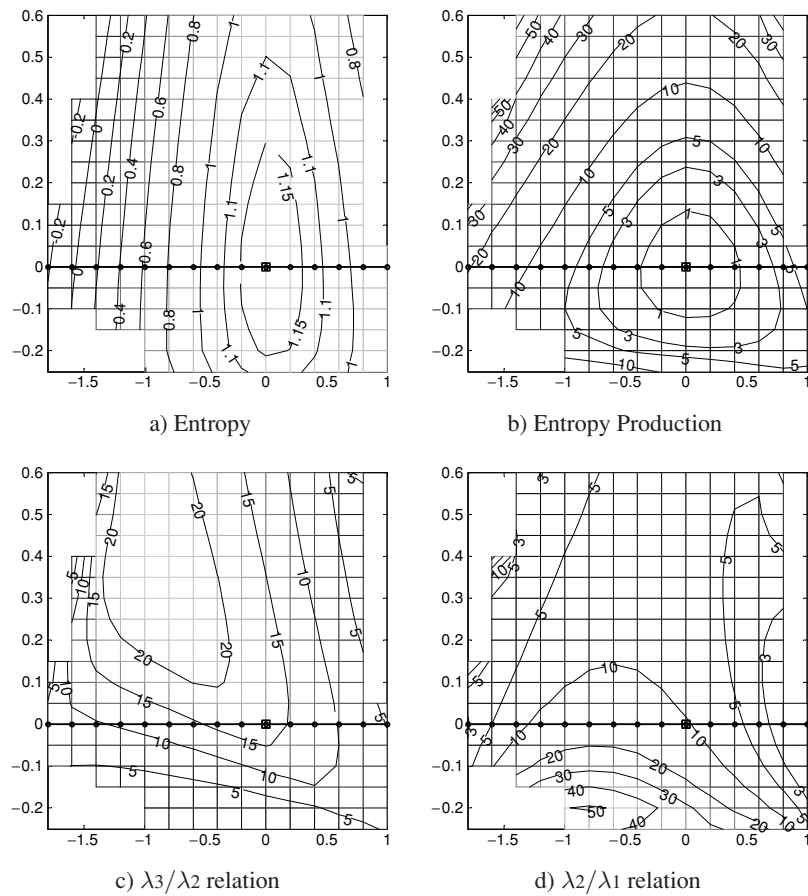


**Fig. 10.7.** Two-dimensional invariant grid as a screen for visualizing different functions defined in the concentrations space. The coordinate axes are entropic distances (see the text for the explanations) along the first and the second slowest directions on the grid. The corresponding 1D invariant grid is denoted by bold line, the equilibrium is denoted by square

Finally, we visualize the relation between the relaxation times of the fast motion towards the 2D-grid and the slow motion along it. This is given on the Fig. 10.7c. This picture allows to make a conclusion that two-dimensional consideration can be appropriate for the system (especially in the “high  $H_2$ , high  $O$ ” region), since the relaxation times “towards” and “along” the grid are well separated. One can compare this to the Fig. 10.7d, where the relation between relaxation times towards and along the 1D-grid is shown.